water

MDPI

Article

Variation of Local Wind Fields under the Background of Climate Change and Its Impact on Algal Blooms in Lake Taihu, China

Yachun Li [1], Shihua Zhu [1], Xin Hang [1], Liangxiao Sun [1], Xinyi Li [2], Xiaochun Luo [3,*] and Xiuzhen Han [4,*]

[1] Jiangsu Climate Center, Nanjing 210009, China; jsqxlyc@163.com (Y.L.); zhu_shihua2021@163.com (S.Z.); hangxin1990@163.com (X.H.); 15005196819@163.com (L.S.)
[2] Nanjing Joint Institute for Atmospheric Sciences, Nanjing 210009, China; lixinyi@cma.gov.cn
[3] Jiangsu Meteorological Service Center, Nanjing 210009, China
[4] National Satellite Meteorological Center, China Meteorological Administration, Beijing 100081, China
* Correspondence: ntlxc9@163.com (X.L.); hanxz@cma.gov.cn (X.H.)

Abstract: Global climate change can greatly promote the continuing expansion of algal blooms in eutrophic inland lakes. Wind fields, an important climate factor, provide an external driving force for the movement of algal blooms. Based on algal bloom satellite imageries and wind observation data from 2003 to 2022, this study explored a quantitative assessment of the variations in surface wind fields and their impacts on the algal blooms in Lake Taihu, China. The results indicate that the mean wind speed at different time scales in the Lake Taihu area presents a continuous descending tendency in recent decades, which is the probable cause for the increasing frequency and severity of algal blooms in the lake. Wind fields affect the formation, location, and severity of algal blooms in diverse and complex ways. The area and frequency of algal blooms in Lake Taihu increase with the decrease in wind speed. The 6 h mean wind speed before 12:00 LT (Local Time) on the day of the algal bloom occurrence generally follows a Gaussian distribution, with a wind speed range of (0.6 m/s, 3.4 m/s) at the 95.5% confidence level. Accordingly, the wind speeds of 0.6 m/s and 3.4 m/s are identified to be the lower and upper critical wind speed indicators suitable for the formation of algal blooms, respectively. Another meaningful finding is that the outbreak of large-scale algal blooms requires stricter wind speed conditions, with a significantly lower wind speed threshold of around 2 m/s. Our study also demonstrates that the dominant wind direction of southeast in the region may be an important cause of the continuous water-quality decline and the high frequency and severity of algal blooms in the northwest waters of the lake. These findings will contribute to further studies on the dynamic mechanism of algal blooms and provide support for water environment management and algal bloom prevention and control.

Keywords: wind field variation; wind speed critical indicator; climate change; algal bloom; Lake Taihu

Citation: Li, Y.; Zhu, S.; Hang, X.; Sun, L.; Li, X.; Luo, X.; Han, X. Variation of Local Wind Fields under the Background of Climate Change and Its Impact on Algal Blooms in Lake Taihu, China. *Water* **2023**, *15*, 4258. https://doi.org/10.3390/w15244258

Academic Editor: Yuqiang Tao

Received: 3 November 2023
Revised: 1 December 2023
Accepted: 4 December 2023
Published: 12 December 2023

1. Introduction

Freshwater, including lakes, rivers, and wetlands, provides vital ecosystem services such as water, food, and energy for human survival [1,2]. However, global freshwater quality has deteriorated and algal blooms have increased in magnitude, frequency, and duration with the combined action of climate warming and human activities over the past decades [3–6]. Some harmful algal blooms can release harmful toxic and odor compounds, which have become a serious problem threatening human health and the stability of freshwater ecosystems [7,8]. Therefore, it is particularly important to adopt scientific strategies to prevent algal blooms and ensure the health of freshwater ecosystems and the safety of drinking water.

There is a broad consensus that climate warming is one of the main driving factors for the increasing intensity and frequency of global algal blooms [4,5,9]. And it is expected

that global algal blooms will continue to increase in the future due to climate warming and extreme climate events increasing [10,11]. However, the interacting mechanism between algal blooms and climate warming as well as freshwater eutrophication, which is a complicated bidirectional mechanism, is yet to be understood at present [8,12–14]. It remains a key challenge we face to determine the potential action mechanisms of climate warming [8].

While algae proliferate and blooms form as a result of various environmental factors [15–18], accumulating evidence has indicated that climate conditions may be the main limiting factor of algal bloom formation when a lake maintains a high level of eutrophication [5,19,20]. Under favorable climate conditions, algal cells can proliferate rapidly and form algal blooms in eutrophic lakes [2]. Climate factors generally affect the number, community, distribution, and life cycle of algae directly or indirectly [4,21]. Some climate factors, such as temperature, wind, precipitation, solar radiation, and atmospheric pressure, have important effects on the proliferation of algae and the formation, expansion, and duration of blooms [22–25]. However, their exact action mechanism triggering and regulating the algal bloom remains largely unclear due to the scarcity of long-term continuous observations [8,26,27].

Many efforts have been made in recent years to explore the dynamic mechanism of wind on algal blooms. Although the algae biomass size is not determined by external factors in essence, wind fields can increase the availability of light, heat, and nutrients by affecting water mixing, heat stratification, transfer and exchange, and the upwelling of nutrients [21,28,29]. The wind and wind-induced currents play critical roles in the floating–sinking process of algae and the variability of algae biomass will increase with increasing variability in wind speed [19,30]. Continuous or strong winds can not only directly disperse algal blooms, but also alter the distribution of nutrients over a longer time scale by eroding density gradients and deepening mixing, leading to changes in biomass concentration [31]. In large shallow eutrophic lakes, winds have even become the decisive factor in the formation, location, and severity of algal blooms [21,31,32]. Wind-induced hydrodynamics not only control the vertical movement of algal colonies but also control their horizontal migration and alter their spatial distribution patterns [29,33]. Under the influences of wind-induced hydrodynamic forces, algal blooms exhibit high spatio-temporal heterogeneity and rapid changes [34–36]. So far, almost all previous studies tend to believe that lower wind speed is conducive to the formation of algal blooms [37,38]. However, wind affects algal blooms in diverse and complex ways at different stages of algae reproduction and bloom formation. In particular, few studies have taken into account the impact of declined wind speeds in certain regions (another consequence of global warming) on algal blooms [39].

The aim of this study is to quantitatively evaluate the near-surface wind field changes under the background of climate warming and the impact of wind fields at different time scales on algal blooms, taking Lake Taihu, China as an example. The rest of this paper is structured as follows. Section 2 describes the study region and the data sources, and Section 3 presents the evaluation results of wind field changes and their impacts on algal blooms. A discussion is presented in Section 4, and concluding remarks are provided in Section 5.

2. Materials and Methods

2.1. Study Area and Data

Lake Taihu (30°5′–32°8′ N, 119°8′–121°55′ E), located in the Yangtze River Delta, one of the most economically and socially developed region in China, is the third-largest freshwater lake in China with an area of approximately 2338 km^2 and an average depth of 1.9 m (Figure 1). This lake is the most important drinking water source in the region, providing water to 10 million residents in the surrounding cities such as Suzhou, Wuxi, and Huzhou. It also provides important ecosystem support for the sustainable and high-quality development of the Yangtze River Delta. Since the 1980s, due to the rapid increases in external nutrient loadings brought by industry, agriculture, and tourism in the watershed,

Lake Taihu has been in a significant eutrophic state, leading to frequent and intensified algal blooms [40]. For example, the large-scale outbreak of algal blooms in the lake in the spring of 2007 caused water pollution, directly affecting the drinking water of millions of people [40]. The observations showed that the proportion of blue algae blooms (including *Microcystis aeruginosa*, *Pseudanabaena* sp., and *Aphanizomenon* sp.) in Lake Taihu is higher than that of green algae (including *Chlorella* sp. and *Scenedesmus quadricauda*) in summer and winter [41]. Under specific wind field conditions, this dominant algae population can quickly change its vertical and horizontal position and "instantly" form algal blooms [36,42]. In recent decades, despite significant progress in the comprehensive management of the water environment within the watershed, eutrophication and frequent algal blooms remain the main ecological problems facing Lake Taihu and present hidden dangers that threaten the urban water supply and ecological security of this region.

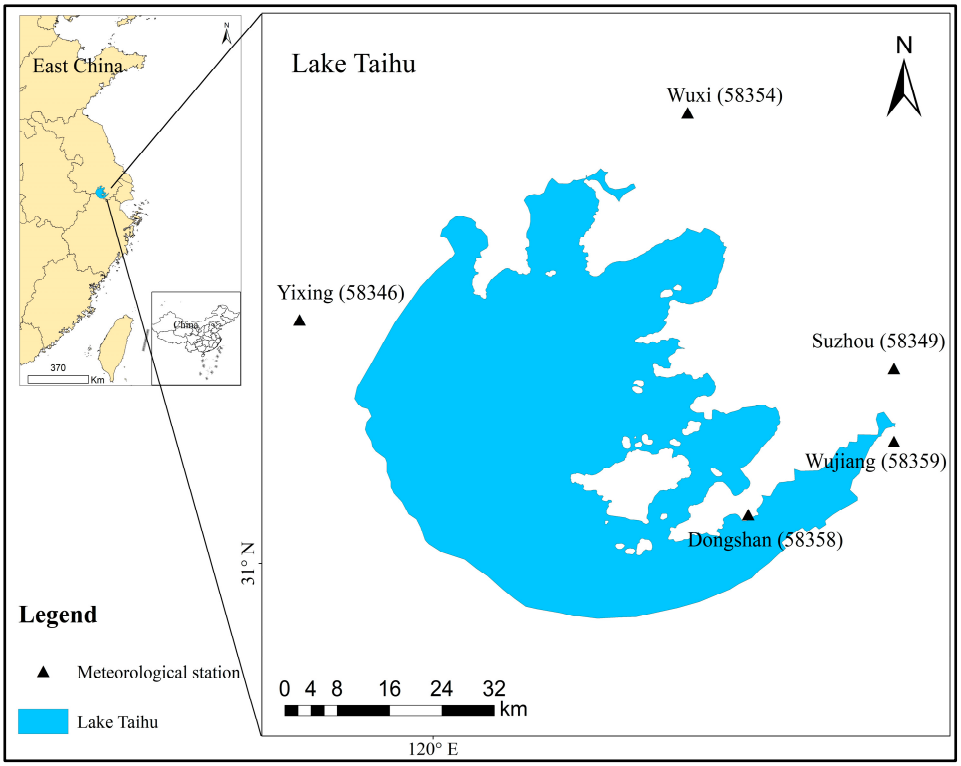

Figure 1. Location of Taihu Lake and surrounding national basic meteorological stations in China.

The satellite data were collected from the National Satellite Meteorological Center, Beijing, China and the Jiangsu Provincial Meteorological Information Center, Nanjing, China. A total of 17,200 MODIS/AQUA, MODIS/Terra, and MERSI/FY3 images from 2003 to 2022 were used in this study for the retrieval of algal blooms. Before this, it was required to preprocess these satellite images, such as resampling to 250 m resolution and removing Rayleigh molecular scattering effects and cloud effects. The meteorological observation data used in this study were from the Jiangsu Provincial Meteorological Information Center. The hourly wind speed and wind direction data from 2003 to 2022 were collected from the five national basic meteorological stations around Lake Taihu, including the Yixing, Wuxi, Suzhou, Wujiang, and Dongshan stations (Figure 1).

2.2. Remote Sensing Retrieval Method for Algal Blooms

The dense algal blooms have spectral reflectance characteristics similar to those of land-based vegetation (red-edge effect), i.e., showing very low reflectivity values in the red band and noticeably high values in the NIR (near-infrared) band with increasing chlorophyll concentration, which is the main theoretical base algal bloom remote sensing retrieval [43]. Similar spectral reflection curves of water, dense algal blooms, and algae-water were also

obtained from field measurements in Lake Taihu, as shown in Figure 2 [44]. According to the algal spectral characteristics, pixels in satellite images containing algae can be identified using several vegetation indexes such as the EVI (Enhanced Vegetation Index), NDVI (Normalized Difference Vegetation Index), and FAI (Floating Algae Index), which include red light and near-infrared bands [45–47]. Here, we adopted the most commonly used NDVI for the inversion of algal blooms, and it can be calculated as follows [43,48]:

$$NDVI = \frac{\rho_{NIR} - \rho_{RED}}{\rho_{NIR} + \rho_{RED}} \quad (1)$$

where $NDVI$ is the NDVI value, ρ_{NIR} and ρ_{RED} are the reflectances of NIR and red light, respectively. The $NDVI$ ranges from -1 to 1, with a smaller value indicating a lower density of algal blooms, while a larger value indicates a higher density of algal blooms.

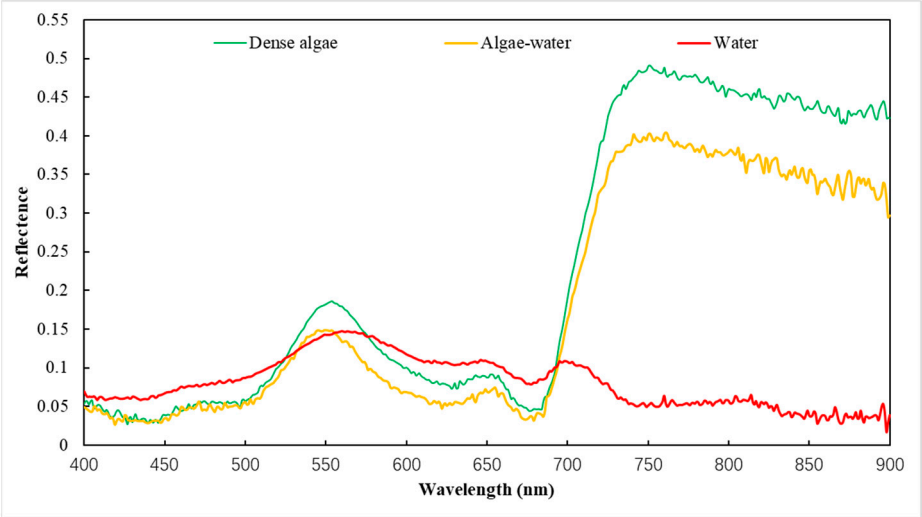

Figure 2. Field measurement reflectance spectra of dense algae, algae-water, and water in Lake Taihu. The spectra values were determined as the average spectra of the three types of observation targets [48].

To determine an appropriate NDVI threshold for detecting algal blooms, a method integrating visual analysis with statistics, a commonly used method for threshold selection, was used in this paper [48]. Firstly, boundaries of algal blooms and water were manually determined in RGB (Red-Green-Blue) imagery containing algal blooms. Then, the mean NDVI value of all pixels along the boundaries was calculated and the mean value was adopted to be the NDVI threshold for detecting algal blooms in this image. According to this method, 1973 images with bloom areas $\geq$1 km^2 were obtained from the 17,200 satellite images of Lake Taihu from 2003 to 2022.

The fractional vegetation cover index, an important parameter for the characterization of the surface vegetation cover [49,50], was adopted in this paper to evaluate the coverage degree of algal blooms. A few studies used this index to present the coverage of lower plants such as tundra [51]. Following the definition of fractional vegetation cover [24,52], we defined the fractional algae cover index (FAC) as the proportion of algal blooms at the lowest point, which can reflect the area size for photosynthetic and coverage density of algal blooms. Assuming that a pixel on the lake surface is always composed of algae and water proportions, the NDVI of a mixed pixel can be expressed as the following equation [48]:

$$NDVI_i = FAC_i \times NDVI_{algae} + (1 - FAC_i) \times NDVI_{water} \quad (2)$$

where the $NDVI_i$ is the NDVI value of the ith mixed pixel, FAC_i and $(1 - FAC_i)$ represent the cover area of the algal blooms and water in the mixed pixel, respectively. $NDVI_{algae}$

and $NDVI_{water}$ represent the NDVI value of pure algae and pure water pixels, respectively. Then, the FAC_i of a mixed pixel can be obtained as follows:

$$FAC_i = (NDVI_i - NDVI_{water})/(NDVI_{algae} - NDVI_{water}) \quad (3)$$

Here, the $NDVI_{algae}$ and $NDVI_{water}$ were determined by calculating cumulative frequencies of NDVI in the image, i.e., the NDVI value with a cumulative frequency of 95% is considered $NDVI_{algae}$ and the NDVI value with a cumulative frequency of 5% is considered $NDVI_{water}$ [52]. In this paper, $NDVI_{algae}$ and $NDVI_{water}$ values were determined as 0.81 and −0.2, respectively [48]. To represent the intensity of algal blooms in the image, according to the size of FAC of each pixel, the algal bloom intensity of each pixel was subjectively divided into four levels: algae-free, slight, moderate, and severe (Table 1).

Table 1. Algal bloom intensity levels according to FAC_i in each pixel.

Levels of Algal Bloom Intensity	FAC_i in Each Pixel
Algae-free	$FAC_i = 0$
Slight	$0 < FAC_i \leq 30\%$
Moderate	$30\% < FAC_i \leq 60\%$
Severe	$60\% < FAC_i \leq 100\%$

We can determine the intensity and distribution of algal blooms in the lake at that time by calculating the algal bloom area at different levels in each image as:

$$S_i = \sum_{i,j=1}^{n} s_{i,j} \quad (4)$$

where S_i is the total area of algal blooms at i intensity level in the image, $s_{i,j}$ is the area of the jth pixel with intensity level i, and n is the total number of pixels with intensity level i. The unit of area is km^2.

To further investigate the relationship between the outbreak of large-area algal blooms and wind, we defined a large-area algal bloom (LAalgae) as an algal bloom with an area that exceeds 20% of the surface area of Lake Taihu or exceeds 468 km^2 in an image. A total of 113 image samples of large-area algal blooms were obtained from all years except 2003 and 2014.

2.3. Statistical Methods for Wind

Firstly, the annual, seasonal, monthly, and daily mean wind speeds (MWS) of the five national basic observation stations around Lake Taihu from 2003 to 2022 were counted, and then the average wind speed in Taihu Lake area on each time scale was calculated.

The transit time of polar-orbiting satellites such as Terra, Aqua, and FY-3 is around local noon, which is also the time when these satellites observed algal blooms. But, in fact, this time is not the time when algal blooms began to appear, nor is it the time when they disappeared. The algal blooms are not formed "instantaneously" on the surface at the moment of satellite transit, but rather, during a period of time prior to this, the accumulated algae biomass floats and agglomerates to form algal blooms when encountering suitable meteorological conditions [42]. In addition, due to the fact that the wind speed in the afternoon is usually the highest of the day, algal blooms often appear in the morning and dissipate in the afternoon, which is currently a popular view [32]. Therefore, we selected the mean wind speed of 6 h (MWS6) during 6:00–12:00 LT (local time) on the day when algae blooms were observed to investigate the influence of winds on the formation of algal blooms. We believe that the MWS6 is more reasonable to represent the wind field suitable for algal bloom formation than the daily MWS. In addition, the wind directions in Lake Taihu were represented by the observed wind direction data from Dongshan Station on the island in the lake.

2.4. Numerical Simulation Method for Near-Surface Wind Fields

To further evaluate the impacts of near-surface wind field changes on algal blooms, the wind field in the Lake Taihu area was simulated using the weather research and forecasting model (WRF). The WRF is a mesoscale numerical weather forecasting model that can simulate meteorological elements with high spatio-temporal resolution, developed by the National Center for Atmospheric Research (NCAR) and the National Center for Environmental Forecasting (NCEP) in the United States of America [53]. In this study, WRF 3.8.1 was used to simulate the near-surface wind field from 08:00 on 3 September to 08:00 on 8 September 2010. During this period, the algal blooms in Lake Taihu experienced an obvious process of growth and decline. The WRF 3.8.1 mode adopts a three-layer nested structure, with grid spacing of 30, 10, and 3.3 km, respectively, and grid points of 232 × 172, 166 × 121, and 109 × 79, respectively. The initial field and boundary meteorological data of the simulation scheme were obtained from FNL (Final Operational Global Analysis) global re-analysis data provided by NCEP with a spatial resolution of 1° × 1° and a time interval of 6 h. The model adopts the Purdue Lin cloud micro-physical parameterization scheme, the Rapid Radiative Transfer Model (RRTM) longwave radiation scheme, the Dudhia shortwave radiation scheme, the Noah land surface model, the GrellDevenyi cumulus parameterization scheme, and the MellorYamada Janjic planetary boundary layer scheme.

3. Results

3.1. Temporal Distribution of Algal Blooms in Lake Taihu

According to the above-mentioned method, a total of 1973 images with algal bloom areas $\geq$1 km^2 were obtained from the satellite images during the period 2003–2022. According to Formula (4), we retrieved the area of algal blooms from each image and calculated the cumulative area for each month, season, and year. As shown in Figure 3, the monthly and yearly cumulative area of algal blooms in Lake Taihu has generally increased with time over the past 20 years. The monthly cumulative area of algal blooms in the lake represented a very obvious periodic change feature, in which the algal blooms usually occurred frequently over the period May–October, but seldom from November to April of the next year (Figure 3a). The monthly cumulative area curves of algal blooms showed a bimodal shape with peak values located at 2007–2008 and 2017–2022. From the inter-annual distribution map of the algal bloom cumulative areas (Figure 3b), we can find that the double-peak characteristics are more obvious, with peaks located in 2007 and 2017. Specifically, the yearly cumulative area continued to increase from 2003 to 2007, reaching its first peak in 2007, and then began to decrease and fluctuate at a relatively low level until reaching its second peak in 2017, which was also the largest cumulative area since 2003. Afterward, the cumulative area began to show a decreasing trend in fluctuations again. The inter-annual differences in cumulative area were significant, with relatively large areas in 2006, 2007, 2017, 2019, and 2020, with an anomalous percentage of over 30%. The cumulative area anomalous percentages in 2003, 2004, 2009, and 2014 were all below −30%.

Similar to the trend of cumulative area, the frequency (frequency indicates the number of algal bloom days) of algal blooms in Lake Taihu also showed a continuous increase over time. From the monthly algal bloom frequencies shown in Figure 4a, it can be seen that the frequencies displayed a continuously increasing tendency. This continuously increasing trend with time of algae bloom frequency was more evident on the annual frequency distribution diagram (Figure 4b). It is worth noting that since the algal bloom frequency exceeded 100 times for the first time in 2013, the algal bloom frequency has exceeded 100 times in 9 out of 10 years. In general, the algal blooms in Lake Taihu presented a sustained expansion tendency in the past 20 years, both in terms of area and frequency.

FAC values of each image with algal blooms were calculated and divided into three levels: mild, moderate, and severe according to the criteria represented in Table 1, and then the cumulative area was calculated for each level. The algal bloom cumulative area at different levels in Lake Taihu over the period 2003–2022 was counted, as shown in Figure 5. We can find that in the past 20 years, the algal blooms were mainly at a slight

level, accounting for 67% of the total areas, and moderate and severe areas accounted for 28% and 5%, respectively. Specifically, the algal bloom area proportion of the slight level in other years fluctuated around 70% and did not show an obvious temporal trend, except for 2008 and 2009, which were significantly lower. Similarly, there was no obvious temporal trend in the area proportion of moderate and severe levels.

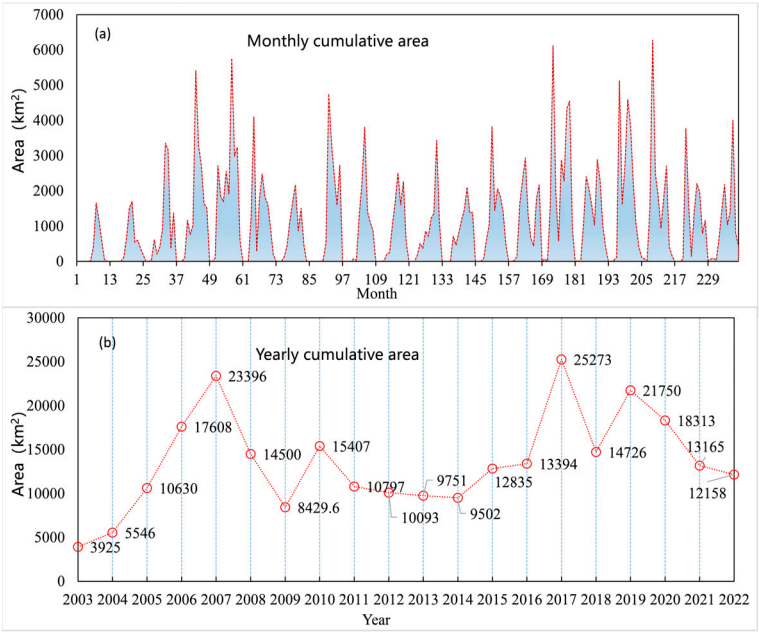

Figure 3. Monthly (**a**) and yearly (**b**) algal bloom cumulative areas in Lake Taihu from 2003 to 2022.

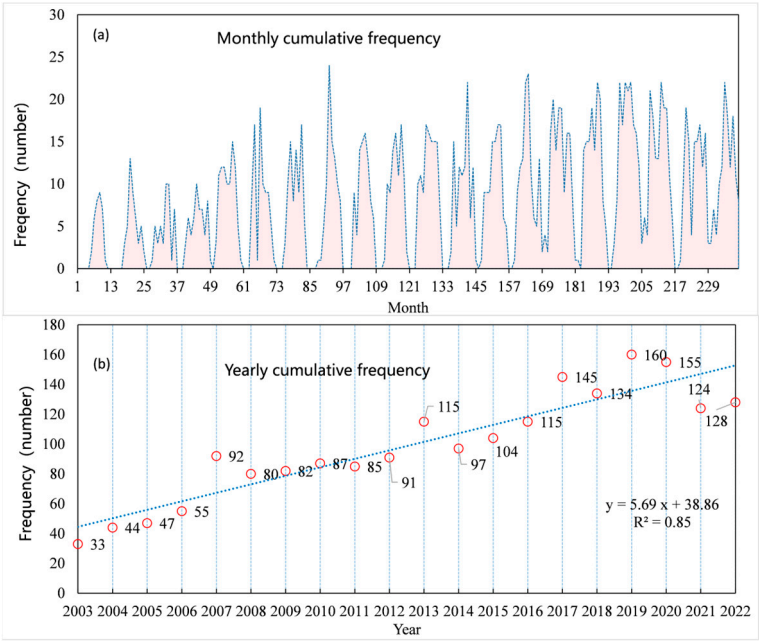

Figure 4. Monthly (**a**) and yearly (**b**) algal bloom cumulative frequencies in Lake Taihu during 2003–2022. The blue dotted line in Figure (**b**) is the trend line of the cumulative frequency.

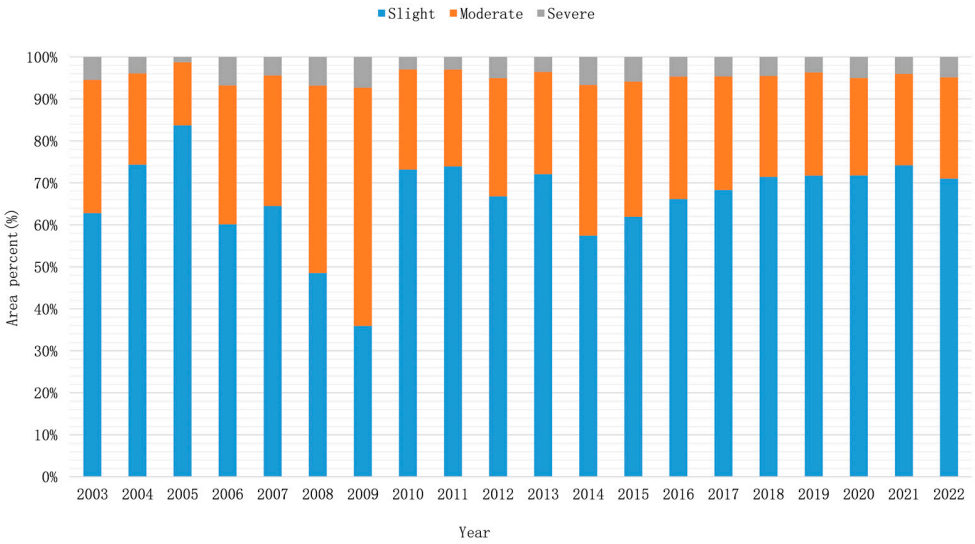

Figure 5. Algal bloom area percentage at slight, moderate, and severe levels in Lake Taihu during 2003–2022.

3.2. Observational Facts of Near-Surface Wind Speed Change

The observations showed that the surface wind speeds in the Lake Taihu area presented an obvious downward trend in the past 20 years (Figure 6). According to the statistical results from the five meteorological stations along Lake Taihu, the regional annual MWS was 2.37 m/s during the period 2001–2022, of which the MWS in 2001 was the largest, reaching 3.14 m/s, and that in 2019 was the smallest, only 1.99 m/s. Our analysis also showed that the annual MWS decreased significantly at a rate of 0.4 m/s (or 16.9%) per decade over the past 20 years starting from 2001 (Figure 6a). However, the wind direction in this area did not obviously change in the past 20 years, with a dominant wind direction of southeast. Similar to the changing trends of mean annual wind speed, seasonal MWS during 2001–2022 also experienced a significant downward trend (Figure 6b–e). The MWS in Spring, Summer, Autumn, and Winter were 2.7 m/s, 2.5 m/s, 2.2 m/s, and 2.3 m/s, respectively. And the average wind speeds in Spring, Summer, Autumn, and Winter during the period 2001–2022 decreased at rates of 0.45 m/s, 0.42 m/s, 0.34 m/s, and 0.44 m/s per decade, respectively.

Here, we will discuss the changes in wind speed in the Lake Taihu area on a monthly time scale. Figure 7a is a heat map of mean monthly wind speed, showing the continuous decline tendency of wind speed in this area in the past 20 years. Specifically, the mean monthly wind speeds began to decrease significantly in January and October–December starting from 2004 and remained relatively low until 2022. The average wind speed in February and June–September decreased significantly after 2007, while that in April–May did not begin to decrease significantly until 2018. It should be noted that the period May–October is usually the most frequent stage of algal blooms in Lake Taihu. Therefore, it seems to be a reasonable deduction that the continuous decrease in wind speed during this period may also be one of the main factors leading to the increase in frequency and intensity of algal blooms in recent years.

Figure 7b is the scatter plot of monthly MWS, mean maximum wind speeds, and mean minimum wind speeds of the five national basic meteorological stations around the lake from 2001 to 2022, displaying the trend of surface wind speeds in the area on a monthly time scale over time since this century. The monthly MWS, mean maximum wind speeds, and mean minimum wind speeds have shown an obviously fluctuated downward trend over the past 20 years. It is particularly important to note that from 2001 to 2006, the monthly mean minimum wind speeds decreased at a very steep slope, with a decline rate significantly higher than other periods. At the same time, we also noticed that the algal bloom area gradually increased beginning from 2003, until large-scale algal blooms

occurred continuously in 2006–2007 (Figure 3). This coincidence of time nodes makes it reasonable to speculate that the continuous decline in the wind speeds, especially the rapid decline in the minimum wind speeds, may be an important trigger factor for the large-scale outbreaks of algal blooms in Lake Taihu since 2006.

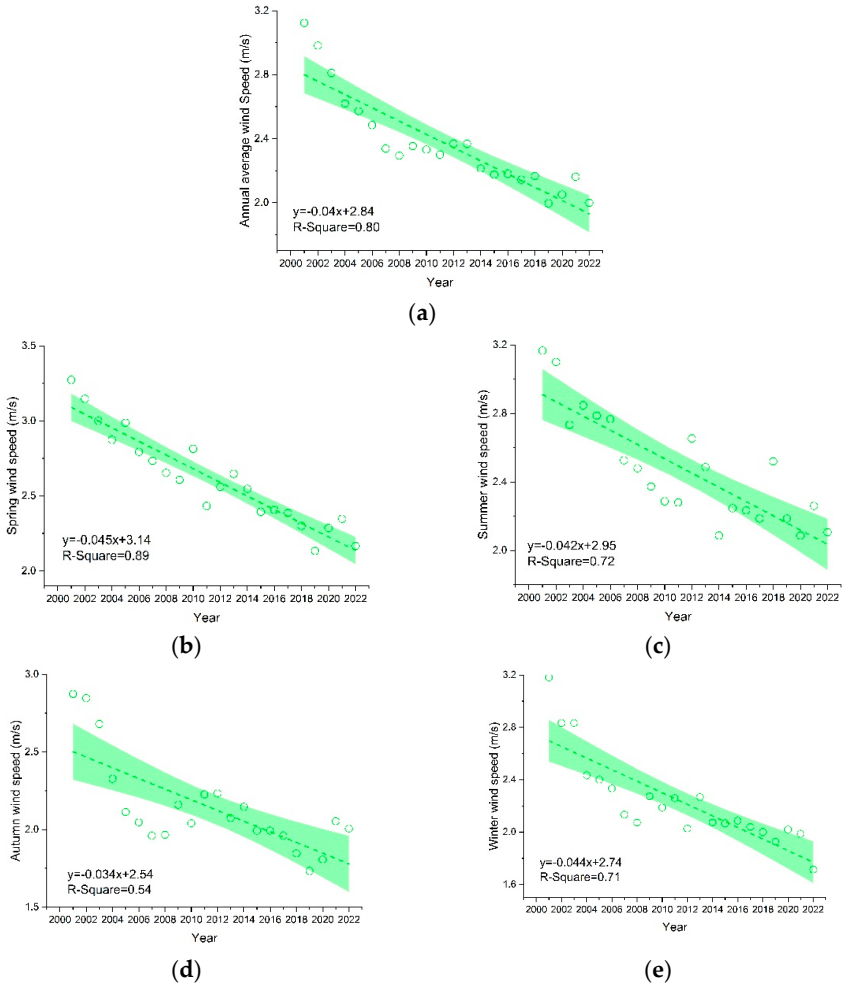

Figure 6. Mean wind speed variation in (**a**) year, (**b**) Spring, (**c**) Summer, (**d**) Autumn, and (**e**) Winter in the Lake Taihu area during 2001–2022. The shadows represent the 95% confidence interval of the linear regression trend line.

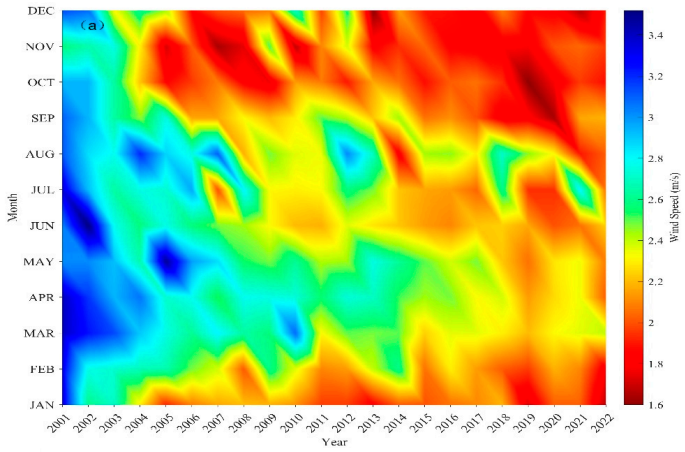

Figure 7. *Cont.*

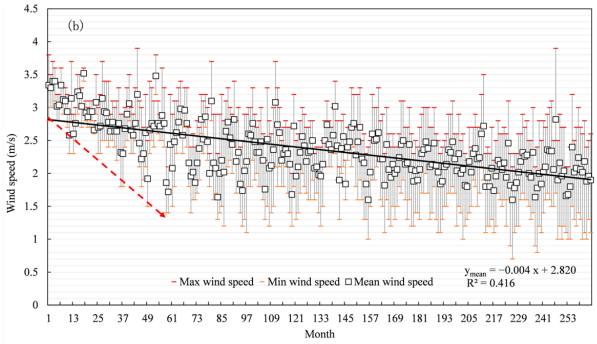

Figure 7. Monthly mean wind speeds in the Lake Taihu area during 2001–2022. Figure (**a**) is the heat map of mean monthly wind speed, showing the decline tendency of wind speed in the past 20 years. The black solid line in Figure (**b**) is the trend line of monthly mean wind speed, while the red dashed line schematically represents the trend of monthly minimum wind speed during 2001–2006.

3.3. The Relationship between Wind Speed and Algal Blooms

Existing research has confirmed that wind and wind-induced currents provide direct power for the accumulation and dissipation, and horizontal and vertical movement of algal communities, and appropriate wind speeds can promote the formation of algal blooms. However, this does not mean that higher wind speeds are more beneficial to the formation of algal blooms. In fact, the cumulative area and frequency of algal blooms were generally negatively correlated with wind speeds from the results we observed. Figure 8 shows the area of 1973 algal bloom samples in Lake Taihu during 2003–2022 and the corresponding MWS6. As can be seen from the figure, the outer contour of the algal area dots displays an approximate right triangle, indicating that the wind speed corresponding to the algal blooms with larger areas is relatively small. However, it is very obvious that no algal bloom was observed by satellites when MWS6 < 0.5 m/s, indicating that wind speed conditions close to calm were not beneficial for the formation of algal blooms due to lack of external dynamics. By dividing all the algal bloom samples into five equal parts and distinguishing them by different colors, it can be found that most of the algal blooms in Lake Taihu occurred in a small area, of which 60% is less than 108 km^2, less than 5% of the surface area of the lake, but its corresponding wind speed range is larger than that of the larger area of algal blooms. Approximately 20% of the algal bloom area did not exceed 15 km^2 but corresponded to the maximum wind speed range (0.8–5.3 m/s).

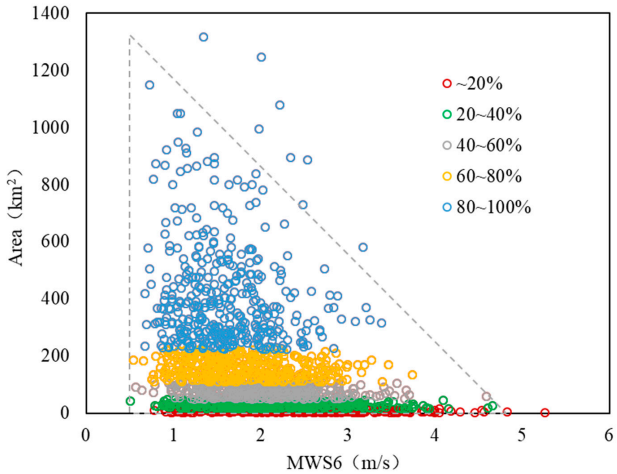

Figure 8. Distribution of bloom areas and corresponding MWS6 (mean wind speed of 6 h during 6:00–12:00 LT) in Lake Taihu during 2003–2022. The percentage represents the frequency ratio of algal blooms with marked colors. The dotted line displays an approximate right triangle, indicating that the wind speed corresponding to the algal blooms with larger areas is relatively small.

Figure 9 shows the relationship between yearly MWS and the frequency and area of algal blooms in Lake Taihu during 2003–2022. It can be found that the yearly cumulative area and frequency of algal blooms were significantly (R-Square = 0.31, $p < 0.05$) or extremely significantly (R-Square = 0.84, $p < 0.01$) negatively correlated with the mean yearly wind speed, respectively. This negative correlation also existed between the seasonal or monthly cumulative area and frequency and the average wind speeds.

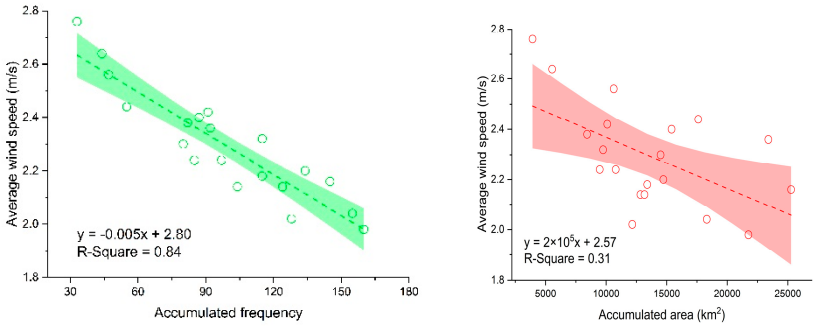

(**a**) (**b**)

Figure 9. Relationship between yearly mean wind speeds and accumulated frequency (R-Square = 0.84, $p < 0.01$) (**a**) and accumulated area (R-Square = 0.31, $p < 0.05$) (**b**) of algal blooms in Lake Taihu during 2003–2022. The shadows represent the 95% confidence interval of the linear regression trend line.

Next, we will discuss the response of different-scale algal blooms to wind speed. We arranged 1973 algal bloom samples in ascending order of area size and divided them into 10 sub-intervals with equal sample number and obtained the area range of algal blooms in each sub-interval as 0–7, 8–15, 16–27, 28–48, 49–75, 76–109, 110–152, 153–224, 225–366, and 367–1317 km^2, respectively. The maximum, minimum, median, upper quartile, and lower quartile of MWS6 within each sub-interval were calculated and represented in the boxplot (Figure 10). We can find that as the area increased, the maximum wind speed in the sub-interval showed a significant downward trend, while the minimum wind speed slowly declined, and the fluctuation ranges generally showed a narrowing trend. The wind speed ranges corresponding to the upper and lower quartiles of wind speeds also narrowed as the area increased. The upper quartile wind speeds decreased from 2.99 m/s, corresponding to the minimum area sub-interval, to 1.88m/s, corresponding to the maximum area sub-interval, by 37.1%. The lower quartile wind speeds declined from 1.92 m/s to 1.18 m/s as the area increased by 38.5%, and the difference in box wind speed decreased from 1.11 m/s to 0.7 m/s, by 36.9%.

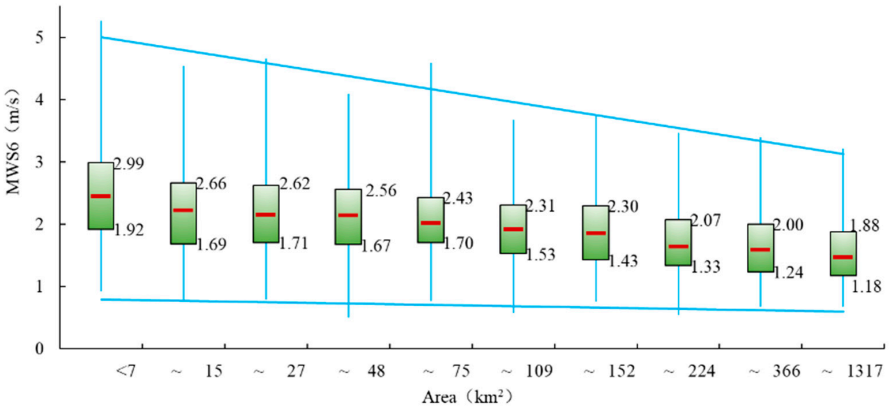

Figure 10. Different algal bloom area sub-intervals and corresponding MWS6 (mean wind speed of 6 h during 6:00–12:00 LT) boxplot during the period 2003–2022. The red line indicates the median, and the bottom and top edges of the box indicate lower quartile and upper quartile, respectively.

A total of 113 LAalgae (large-area algal bloom with an area exceeding 468 km^2) image samples were obtained for assessing the impacts of surface wind on large-scale algal blooms. Figure 11 displays the relationship between LAalgae frequency and MWS6. The wind speed range is divided into 10 equal parts in the figure. It was found that the LAalgae with the highest frequency was observed in the wind speed range of (1.1–1.3 m/s], accounting for 20.4%. LAalgae mainly occurred in the wind speed range of (0.7–2.3 m/s), accounting for 96%. It was obvious that the wind speed range for the formation of LAalgae was significantly narrower than that for the general algal blooms. Moreover, the maximum wind speed of about 2 m/s for LAalgae occurrence was much smaller than the speed of about 3 m/s for general algal blooms. It indicated that the LAalgae can only occur under more strict wind speeds with MWS6 less than about 2 m/s. The wind dynamics can drive small algal patch aggregation to form a larger area of algae blooms, as well as disperse the large area of blooms to small patches. Overall, wind speed had a negative effect on the area of algae blooms, and the smaller the wind speed, the greater the probability of forming a larger-scale algal bloom.

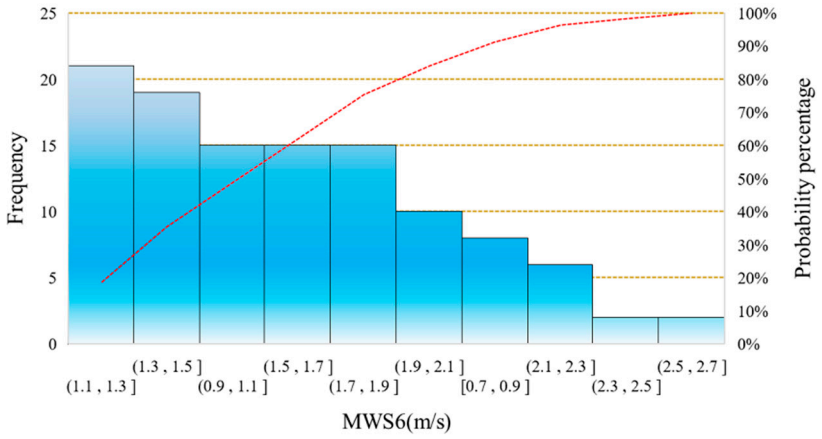

Figure 11. Frequency and probability percentage of LAalgae (algal bloom with an area exceeding 468 km^2) at different MWS6 (mean wind speed of 6 h during 6:00–12:00 LT) sub-intervals during 2003–2022. The red dotted line indicates the accumulated probability percentage.

3.4. Response of Algal Blooms to Near-Surface Wind Fields

The wind direction mainly affects the distribution pattern of algal blooms in the entire lake by regulating the transport direction of nutrients within the lake and the movement direction of surface algal blooms. Figure 12 shows the spatial distribution pattern of algal bloom frequency in Lake Taihu and the wind rose diagram of the region in the past 20 years. We found that the spatial distribution pattern of algal blooms in the lake presented an obvious gradient structure, with the highest frequency of algal blooms appearing in the northwest near-shore waters and gradually decreasing towards the southeast Lake Taihu (Figure 12a). It is particularly interesting to find from the wind rose (Figure 12b) that the dominant wind direction in the Lake Taihu area for decades was southeast. The location with the highest frequency of algal blooms precisely corresponded to the downwind direction of the dominant wind direction. Therefore, this may be a reasonable explanation, that is, under the continuous power provided by the perennial southeast winds throughout the year, algal colonies continue to move towards the northwest direction, accumulating and forming algal blooms as they approach the lake shore. Moreover, the long-term effects of such wind fields may lead to a vicious circle of water-quality decline and algae outbreaks. Under the influences of prevailing winds, nutrients in the lake continued to accumulate in the northwest waters, leading to a continuous decline in the water quality, making these waters more prone to algal blooms than other areas. At the same time, more algal blooms died and decayed, causing a deterioration of water quality in this area. In fact, the

northwest waters of Lake Taihu have always been the part with the worst water quality over the past decades [54].

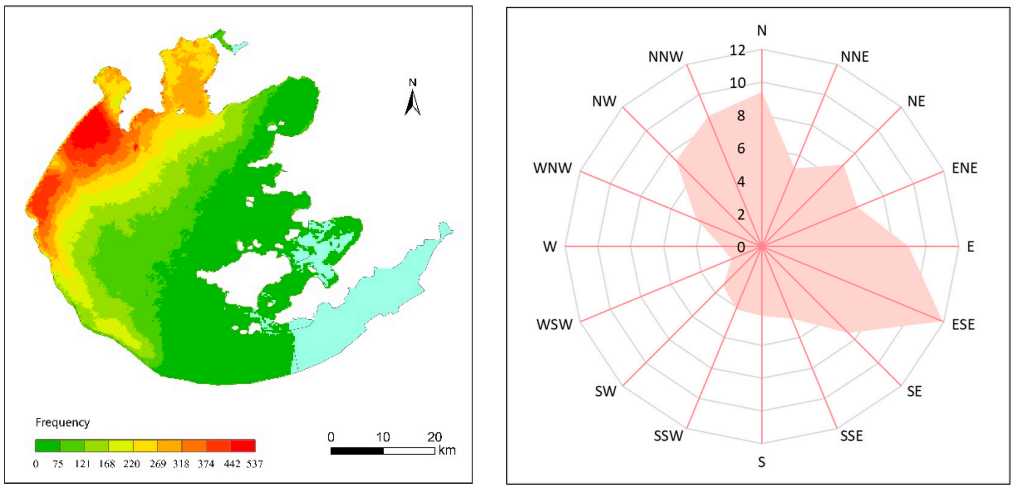

(**a**) (**b**)

Figure 12. The spatial distribution of algal bloom frequency in Lake Taihu (**a**) and the wind rose diagram (**b**) during 2003–2022.

Let us examine in detail how short-term wind fields affect algal blooms. Due to the lack of enough dense lake surface observation data, we could not obtain the actual wind field in the Lake Taihu area. We adopted the weather research and forecasting model (WRF3.8.1), one of the world's most popular numerical weather prediction models supported by the National Center for Atmospheric Research (NCAR), to simulate the wind field near the lake surface in this study. We selected the 4-day period from September 4 to 7, 2010 as an example to simulate the lake surface wind field. The weather conditions in those days in the Lake Taihu area were generally suitable for algal bloom formation and satellites observed algal blooms for four consecutive days. The algal bloom areas and meteorological observation data are shown in Table 2. The algal bloom areas on September 4th and 6th reached 789 km^2 and 795 km^2, with corresponding 1 h average wind speeds of 1.9 m/s and 1.8 m/s, respectively. The algal bloom areas on 5 and 7 September were 67 km^2 and 7 km^2, with corresponding average wind speeds increasing to 2.1 m/s and 2.1 m/s, respectively. This suggested that the changes in wind speed may be the cause of the rapid changes in the algal bloom area on adjacent dates.

Table 2. Algal bloom area and meteorological data from 4 to 7 September 2010. The mean wind speed and average temperature were calculated from the observation data from the five national basic meteorological stations around Lake Taihu.

Time	Mean Wind Speed (m/s)	Average Temperature (°C)	Area (km^2)
4 September, 13:00	1.9	29.7	789
5 September, 10:00	2.1	29.3	67
6 September, 11:00	1.8	28.8	795
7 September, 10:00	2.4	28.8	6

Figure 13 displays the algae bloom intensity interpreted from satellite images on 4–7 September 2010 and the adjacent time wind field near the lake surface simulated by WRF3.8.1. From the intensity map at 13:00 on September 4 (Figure 13(a1)), we can see that the algal blooms covered most of the waters in the middle and north of Lake Taihu, and the areas with greater intensity were concentrated in the waters of the center and north lake, reaching a moderate to severe level. In the simulated wind field map at its adjacent time (Figure 13(b1)), the average wind speeds of the waters where algae blooms occur were less than 3 m/s, significantly lower than those of 4–6 m/s of other waters, with a wind direction

of northeast. In the simulated wind field map at 9:00 on 5 September (Figure 13(b2)), the MWS in the waters where algal blooms appeared the previous day increased, with only the southwest coastal waters experiencing lower wind speeds. Correspondingly, only a small area of algal blooms could be seen in the remote sensing map at 10:00 (Figure 13(a2)), which was blown by northeast winds and drifted to the western coastal waters. In the maps at 9:00 on 6 September (Figure 13(c1,c2)), the wind speeds in the northeast of the lake increased to more than 4 m/s, and those in the southwest were significantly lower. It seems very "magical" that a large area of algal blooms has resurfaced in these waters with relatively low wind speeds. The algal bloom intensity was generally above medium, and at a severe level in nearshore waters due to accumulation. At around 10:00 on 7 September, the wind speed significantly increased, with wind speeds exceeding 4 m/s in most waters, and the algal blooms almost disappeared (Figure 13(d1,d2)). This 4-day example of the "growth and disappearance" process of algal blooms provided a good explanation of how the near-surface wind field affected the movement of algal blooms, thereby affecting their spatial distribution pattern.

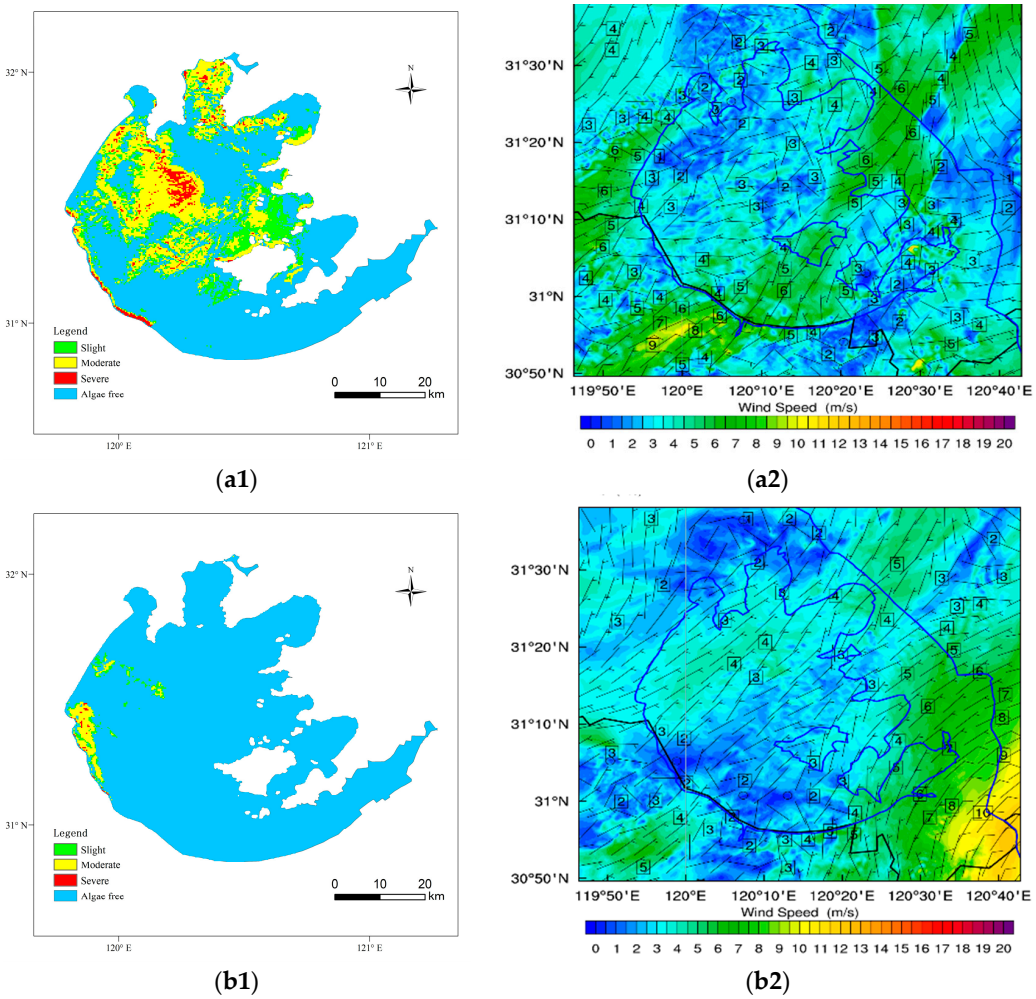

Figure 13. *Cont.*

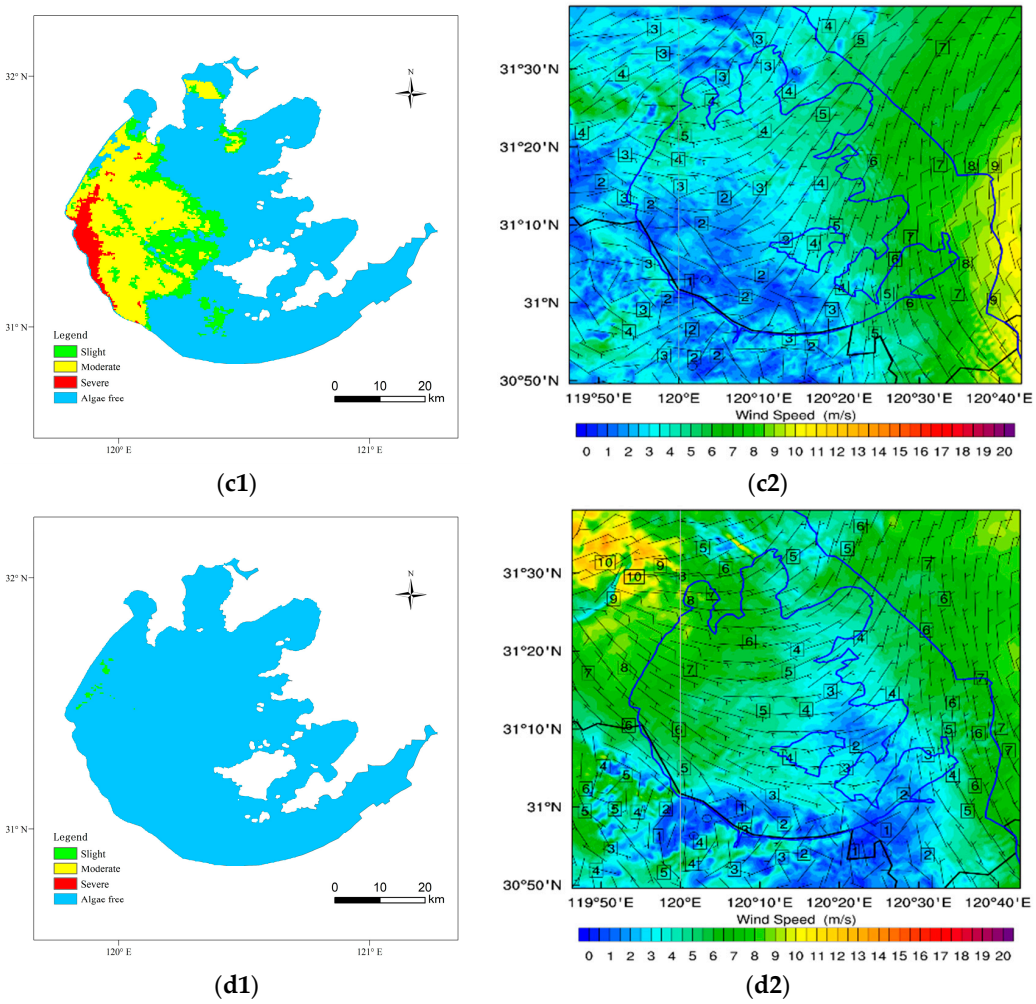

Figure 13. The distribution of algal blooms and the near-surface wind field simulated by WRF3.8.1. The time is around 13:00 on 4 September (**a1**,**a2**), 10:00 on 5 September (**b1**,**b2**), 11:00 on 6 September (**c1**,**c2**), and 10:00 on 7 September (**d1**,**d2**), 2010, respectively. The numbers in Figure (**a2**–**d2**) represent the wind speed (m/s) simulated by WRF3.8.1.

4. Discussion

4.1. The Wind Speed Critical Indicators Suitable for Algal Blooms

Identification of the optimal wind speed critical indicators for suitable algae blooms is of great significance for dynamics research, but also for the prediction, warning, prevention, and control of algal blooms. Many efforts have been made in previous studies to determine the wind speed thresholds suitable for different water bodies. In the simulation experiment of the algae migration model, Wesbster [55] and Zhu et al. [56] estimated that there existed a critical wind speed of 2–3 m/s during the momentum exchange process on the water surface, and the critical value was indicated as the appropriate wind speed threshold for algal blooms. To the best of our knowledge, some subsequent studies established various empirical thresholds similar to this based on some observational data. The thresholds range from 2.0 to 4.5 m/s due to differences in wind speed observation time, selected water bodies, and analysis methods [21,22,57]. In the present study, we will identify the critical indicator of wind speed for algal blooms from a statistical perspective.

By dividing the MWS6 range (0.5–5.3 m/s) corresponding to 1973 algal bloom samples into 20 equal parts, we obtained the cumulative frequency of every sub-interval as shown in Figure 14. Here, the frequency of four MWS6 sub-intervals exceeded 200, each accounting for more than 10% with a cumulative proportion of 50.7%, and four exceeded 100, accounting for 5.6–9.9% with a cumulative proportion of 33.1%. This indicated that the four

sub-intervals with the highest frequency proportion were the most suitable wind speed range for the formation of algal blooms, corresponding to MWS6 ranges of 1.2~2.2 m/s. And 83.8% of algal blooms occurred within the MWS6 range of 1.0~2.9 m/s, which was a suitable wind speed range for the formation of algal blooms. Furthermore, we can find that the frequency histogram of MWS6 approximately exhibited a Gaussian distribution with an average value of 2.0 m/s, and a 95.5% confidence interval of (0.6 m/s, 3.4 m/s). On the basis of this result, it was reasonable that the MWS6 of 0.6 m/s and 3.4 m/s are identified to be the lower and upper critical wind speed indicators suitable for the formation of algal blooms, respectively. The upper limit wind speed of this critical interval is basically consistent with the 3 m/s wind speed estimated by the algae migration model [55,56], which forms, in another sense, mutual corroboration.

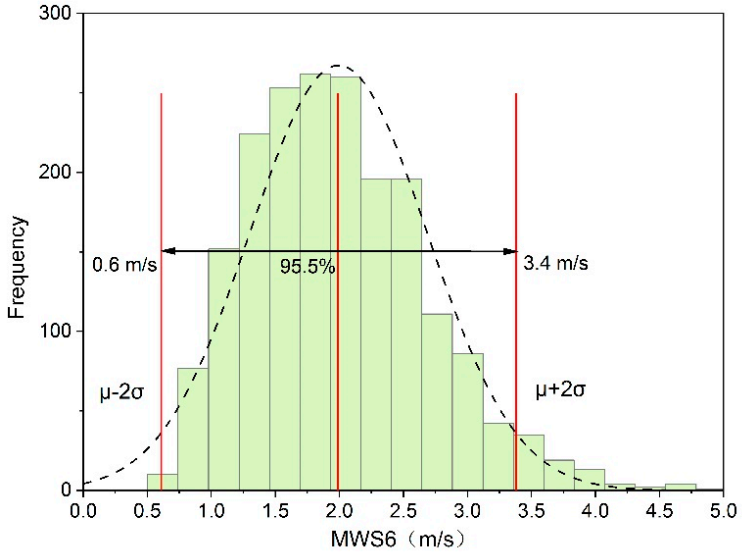

Figure 14. Gaussian distribution of MWS6 (mean wind speed of 6 h during 6:00–12:00 LT) on the days when algal blooms occurred during 2003–2022. The dotted line is Gaussian distribution curve and the red lines represent the μ–2δ, average value and μ+2δ, respectively.

4.2. Implications for Management and Future Research

Another meaningful finding is that the downwind waters of the dominant wind direction in the Lake Taihu region are highly consistent with the waters with the most frequent and severe algal blooms. We infer from this that the long-term prevailing southeast wind continuously gathered the nutrients of the entire lake into the downwind northwest waters, leading to a continuous decline in water quality and triggering algae blooms. The death and decay of algae blooms further led to water quality deterioration, forming a vicious cycle. However, many existing studies have not analyzed the reasons for this phenomenon from a climate perspective, but rather from that of anthropogenic emissions of pollutants [54,58,59]. However, it is not commensurate with the intensive effluent reduction efforts of the government that the algal blooms in Lake Taihu are still serious in recent years, which does not seem to be well explained from the perspective of pollutant emissions [5,24]. Therefore, our findings suggest that the deterioration of water quality and outbreaks of algal blooms in certain waters of a large shallow lake are likely closely related to the dominant wind direction, which is crucial for managers to determine bloom prevention and control measures and formulate water environment management policies.

The stress effects of climate change on algal blooms are not caused by a single climatic factor but rather by the synergies of various climatic factors [21,60]. However, few studies have addressed the comprehensive impacts of these synergies on algae blooms [6,22,35]. The limitations of our research naturally include not considering the synergistic effects of wind fields combined with other climate factors on algal blooms. Therefore, future research should not only further reveal the mechanisms of various single meteorological

factors on algal blooms but also focus on quantitatively evaluating the comprehensive impact of various climate factors and their changes on the sustained expansion of algal blooms. In addition, it is generally believed that in addition to the amplified warming in the northern hemisphere, the increased surface roughness/friction (e.g., the urbanization and greening of the earth) is also another important reason for the decline in near-surface wind speeds [61]. This study only analyzed the fact that the near-surface wind speed changes observed under the background of climate change and the response of cyanobacterial blooms to them and did not specifically discuss the extent to which climate change caused the decline in wind speed, which is also the focus of our future research.

5. Conclusions

Our research indicates that the continuous decline in wind speed under the background of climate change is probably the main external cause of the algal bloom expansion in Lake Taihu in recent decades. The wind speed data corresponding to the occurrence of algal blooms generally present a Gaussian distribution, and the frequency and area of algal blooms increase with the decrease in wind speed within the appropriate wind speed range. The outbreak of large-scale algal blooms requires stricter wind speed conditions, with critical wind speeds significantly lower than those of the algal blooms in general. The dominant wind direction of southeast in the region may be an important reason for the continuous decline in water quality and the high frequency and severity of algal blooms in the northwest waters of the lake. These findings will contribute to further studies on the dynamic mechanism of algal blooms and provide support for water environment management and algal bloom prevention and control.

Author Contributions: Y.L.: Methodology, Writing—original draft, Writing—review and editing, Funding acquisition. S.Z. and X.H. (Xin Hang): Investigation, Data curation. X.L. (Xinyi Li) and L.S.: Validation, Data curation; X.L. (Xiaochun Luo): Formal analysis, Resources; X.H. (Xiuzhen Han): Conceptualization, Funding acquisition. All authors have read and agreed to the published version of the manuscript.

Funding: This study was supported by the National Natural Science Foundation of China (U2242211) and the Foundation for Key Scientific Research of Jiangsu Meteorological Bureau (KZ202003).

Data Availability Statement: The data presented in this study are available on request from the corresponding author.

Acknowledgments: We thank Changyu Hu and Xiang Li for providing IT support.

Conflicts of Interest: The authors declare no conflict of interest.

References

1. Vári, Á.; Podschun, S.A.; Erős, T.; Hein, T.; Pataki, B.; Iojă, I.-C.; Adamescu, C.M.; Gerhardt, A.; Gruber, T.; Dedić, A.; et al. Freshwater systems and ecosystem services: Challenges and chances for cross-fertilization of disciplines. *Ambio* **2022**, *51*, 135–151. [CrossRef]
2. Wang, Q.; Wang, T.; Zhao, S.; Yang, K.; Wen, X.; Zhao, M.; Luo, F.; Jiang, B.; Jin, Y.; Zhang, B. Comprehensive meteorological factors analysis and lag correlation study for cyanobacterial blooms in shallow plateau lake. *Ecol. Indic.* **2023**, *153*, 110394. [CrossRef]
3. Anna, R.; Cayelan, C.C.; Bas, W.I.; Justin, D.B. The interaction between climate warming and eutrophication to promote cyanobacteria is dependent on trophic state and varies among taxa. *Limnol. Oceanogr.* **2014**, *59*, 99–114.
4. Richardson, J.; Feuchtmayr, H.; Miller, C.; Hunter, P.D.; Maberly, S.C.; Carvalho, L. Response of cyanobacteria and phytoplankton abundance to warming, extreme rainfall events and nutrient enrichment. *Glob. Chang. Biol.* **2019**, *25*, 3365–3380. [CrossRef]
5. Qin, B.; Paerl, H.; Brookes, J.; Liu, J.; Jeppesen Erik Zhu, G.; Zhang, Y.; Xu, H.; Shi, K.; Deng, J. Why Lake Taihu continues to be plagued with cyanobacterial blooms through 10 years (2007–2017) efforts. *Sci. Bull.* **2019**, *64*, 354–356. [CrossRef]
6. Luo, A.; Chen, H.; Gao, X.; Laurence, C.; Xue, Y.; Jin, L.; Yang, J. Short-term rainfall limits cyanobacterial bloom formation in a shallow eutrophic subtropical urban reservoir in warm season. *Sci. Total Environ.* **2022**, *827*, 154172. [CrossRef] [PubMed]
7. Huisman, J.; Codd, G.A.; Paerl, H.W.; Bas, W.I.; Jolanda, M.H.V.; Petra, M.V. Cyanobacterial blooms. *Nat. Rev. Microbiol.* **2018**, *16*, 471–483. [CrossRef]

8. Lin, Q.; Zhang, K.; McGowan, S.; Huang, S.; Xue, Q.; Eric, C.; Zhang, C.; Zhao, C.; Shen, J. Characterization of lacustrine harmful algal blooms using multiple biomarkers: Historical processes, driving synergy, and ecological shifts. *Water Res.* **2023**, *235*, 119916. [CrossRef]
9. Visser, P.M.; Verspagen, J.M.H.; Sandrini, G.; Stal, L.J.; Matthijs, H.C.P.; Davis, T.W.; Paerl, H.W.; Huisman, J. How rising CO_2 and global warming may stimulate harmful cyanobacterial blooms. *Harmful Algae* **2016**, *54*, 145–159. [CrossRef]
10. Steven, C.C.; Brent, B.; Charles, F.; Victor, J.; Bierman, J.; Jim, H.; David, M.; Diane, M.L.M.; Lisa, R.; Lesley, J.; et al. Climate Change Impacts on Harmful Algal Blooms in U.S. Freshwaters: A Screening-Level Assessment. *Environ. Sci. Technol.* **2017**, *51*, 8933–8943.
11. Burford, M.A.; Carey, C.C.; Hamilton, D.P.; Huisman, J.; Paerl, H.; Wood WS, A.; Wulff, A. Perspective: Advancing the research agenda for improving understanding of cyanobacteria in a future of global change. *Harmful Algae* **2020**, *91*, 101601. [CrossRef]
12. Yan, X.; Xu, X.; Wang, M.; Wang, G.; Wu, S.; Li, Z.; Sun, H.; Shi, A.; Yang, Y. Climate warming and cyanobacteria blooms: Looks at their relationships from a new perspective. *Water Res.* **2017**, *125*, 449–457. [CrossRef]
13. Cressey, D. Climate change is making algal blooms worse. *Nature* **2017**. [CrossRef]
14. Wang, P.; Ma, J.; Wang, X.; Tan, Q. Rising atmospheric CO_2 levels result in an earlier cyanobacterial bloom-maintenance phase with higher algal biomass. *Water Res.* **2020**, *185*, 116267. [CrossRef]
15. Paerl, H.W.; Otten, T.G. Harmful Cyanobacterial Blooms: Causes, Consequences, and Controls. *Microb. Ecol.* **2013**, *65*, 995–1010. [CrossRef] [PubMed]
16. Bista, D.; Heckathorn, S.A.; Bridgeman, T.; Chaffin, J.D.; Mishra, S. Interactive Effects of Temperature, Nitrogen, and Zooplankton on Growth and Protein and Carbohydrate Content of Cyanobacteria from Western Lake Erie. *J. Water Resour. Prot.* **2014**, *6*, 1139–1153. [CrossRef]
17. Zhang, M.; Shi, X.; Yang, Z.; Yu, Y.; Shi, L.; Qin, B. Long-term dynamics and drivers of phytoplankton biomass in eutrophic Lake Taihu. *Sci. Total Environ.* **2018**, *645*, 876–886. [CrossRef] [PubMed]
18. Luo, X.; Hang, X.; Cao, Y.; Hang, R.; Li, Y. Dominant meteorological factors affecting cyanobacterial blooms under eutrophication in Lake Taihu. *J. Lake Sci.* **2019**, *31*, 1248–1258.
19. Li, W.; Qin, B. Dynamics of spatiotemporal heterogeneity of cyanobacterial blooms in large eutrophic Lake Taihu, China. *Hydrobiologia* **2019**, *833*, 81–93. [CrossRef]
20. Wu, D.; Jia, G.; Wu, H. Chlorophyll-a concentration variation characteristics of the algae-dominant and macrophyte-dominant areas in Lake Taihu and its driving factors, 2007–2019. *J. Lake Sci.* **2021**, *33*, 1364–1375.
21. Zhang, Y.; Loiselle, S.; Shi, K.; Han, T.; Zhang, M.; Hu, M.; Jing, Y.; Lai, L.; Zhan, P. Wind Effects for Floating Algae Dynamics in Eutrophic Lakes. *Remote Sens.* **2021**, *13*, 800. [CrossRef]
22. Li, Y.; Xie, X.; Hang, X.; Zhu, X.; Huang, S.; Jing, Y. Analysis of wind field features causing cyanobacteria bloom in Taihu Lake combined with remote sensing methods. *China Environ. Sci.* **2016**, *36*, 525–533.
23. Qin, B.; Yang, G.; Ma, J.; Wu, T.; Li, W.; Liu, L.; Deng, J.; Zhou, J. Spatiotemporal Changes of Cyanobacterial Bloom in Large Shallow Eutrophic Lake Taihu, China. *Front. Microbiol.* **2018**, *9*, 451. [CrossRef] [PubMed]
24. Jia, T.; Zhang, X.; Dong, R. Long-Term Spatial and Temporal Monitoring of Cyanobacteria Blooms Using MODIS on Google Earth Engine: A Case Study in Taihu Lake. *Remote Sens.* **2019**, *11*, 2269. [CrossRef]
25. Weber, S.J.; Mishra, D.R.; Wilde, S.B.; Kramer, E. Risks for cyanobacterial harmful algal blooms due to land management and climate interactions. *Sci. Total Environ.* **2020**, *703*, 134608. [CrossRef]
26. Rajesh, P.R.; Datta, M.; Aran, I. Bloom Dynamics of Cyanobacteria and Their Toxins: Environmental Health Impacts and Mitigation Strategies. *Front. Microbiol.* **2015**, *6*, 1254.
27. Li, J.; Li, Y.; Dong, X.; Wang, H.; Cai, X.; Zhu, Y.; Lyu, H.; Zeng, S.; Bi, S.; Wang, G. Contributions of meteorology and nutrient to the surface cyanobacterial blooms at different timescales in the shallow eutrophic Lake Taihu. *Sci. Total Environ.* **2023**, *894*, 165064. [CrossRef]
28. Zhu, G.; Qin, B.; Gao, G. Direct evidence of phosphorus outbreak release from sediment to overlying water in a large shallow lake caused by strong wind wave disturbance. *Chin. Sci. Bull.* **2005**, *50*, 577–582. [CrossRef]
29. Qin, B.; Zhang, Y.; Zhu, G.; Gao, G. Eutrophication control of large shallow lakes in China. *Sci. Total Environ.* **2023**, *881*, 163494. [CrossRef] [PubMed]
30. Xue, Z.; Zhu, W.; Zhu, Y.; Fan, X.; Chen, H.; Feng, G. Influence of wind and light on the floating and sinking process of Microcystis. *Sci. Rep.* **2022**, *12*, 5655. [CrossRef]
31. Rusak, J.A.; Tanentzap, A.J.; Klug, J.L.; Rose, K.C.; Hendricks, S.P.; Jennings, E.; Laas, A.; Pierson, D.; Ryder, E.; Smyth, R.L.; et al. Wind and trophic status explain within and among-lake variability of algal biomass. *Limnol. Ocean. Lett.* **2018**, *3*, 409–418. [CrossRef]
32. Qin, B.; Yang, G.; Ma, J.; Deng, J.; Li, M.; Wu, T.; Liu, L.; Gang, G.; Zhu, G.; Zhang, Y. Dynamics of variability and mechanism of harmful cyanobacteria bloom in Lake Taihu, China. *Chin. Sci. Bull.* **2016**, *7*, 12.
33. Cyr, H. Winds and the distribution of nearshore phytoplankton in a stratified lake. *Water Res.* **2017**, *122*, 114–127. [CrossRef] [PubMed]
34. Zhou, J.; Qin, B.; Céline, C.; Han, X.; Yang, G.; Wu, T.; Wu, P.; Ma, J. Effects of wind wave turbulence on the phytoplankton community composition in large, shallow Lake Taihu. *Environ. Sci. Pollut. Res.* **2015**, *22*, 12737–12746. [CrossRef] [PubMed]
35. Qin, B. Shallow lake limnology and control of eutrophication in Lake Taihu. *J. Lake Sci.* **2020**, *32*, 1229–1243.

36. Zhang, Y.; Zhang, Y.; Li, N.; Sun, X.; Wang, W.; Qin, B.; Zhu, G. Capturing the rapid intra-day change of cyanobacteria bloom by land-based hyperspectral remote sensing in Lake Taihu. *J. Lake Sci.* **2021**, *33*, 1951–1960.
37. Wu, D.; Chen, F.; Hu, J.; Ji, G.; Shi, Y.; Shen, A. The declining cyanobacterial blooms in Lake Taihu (China) in 2021: The interplay of nutrients and meteorological determinants. *Ecol. Indic.* **2022**, *145*, 109590.
38. Li, J.; Liu, Y.; Xie, S.; Li, M.; Chen, L.; Wu, C.; Yan, D.; Luan, Z. Landsat-Satellite-Based Analysis of Long-Term Temporal Spatial Dynamics of Cyanobacterial Blooms: A Case Study in Taihu Lake. *Land* **2022**, *11*, 2197. [CrossRef]
39. Mohammad, H.R.; David, P.H.; Amir, E.; Fernanda, H. Impacts of atmospheric stilling and climate warming on cyanobacterial blooms: An individual-based modelling approach. *Water Res.* **2022**, *221*, 118814.
40. Shi, K.; Zhang, Y.; Zhou, Y.; Liu, X.; Zhu, G.; Qin, B.; Gao, G. Long-term MODIS observations of cyanobacterial dynamics in Lake Taihu: Responses to nutrient enrichment and meteorological factors. *Sci. Rep.* **2017**, *7*, 40326. [CrossRef] [PubMed]
41. Zhu, Y.; Li, Y.; Zhang, Y.; Wang, H.; Cai, X.; Cheng, X.; Lv, H. Identification of dominant algae in Lake Taihu based on remote sensing reflectance. *J. Lake Sci.* **2023**, *35*, 73–87.
42. Kong, F.X.; Ma, R.H.; Gao, J.F.; Wu, X.D. The theory and practice of prevention, forecast and warning on cyanobacteria bloom in Lake Taihu. *J. Lake Sci.* **2009**, *21*, 314–328.
43. Feng, L. Key issues in detecting lacustrine cyanobacterial bloom using satellite remote sensing. *J. Lake Sci.* **2021**, *33*, 647–652.
44. Han, X.Z.; Wu, C.Y.; Zheng, W.; Sun, L. Satellite remote sensing of Cyanophyte using observed spectral measurements over the Taihu lake. *J. App. Met. Sci.* **2012**, *21*, 724–730.
45. Duan, H.T.; Zhang, S.X.; Zhang, Y.Z. Cyanobacteria bloom monitoring with remote sensing in Lake Taihu. *J. Lake Sci.* **2008**, *20*, 145–152.
46. Tucker, C.J. Red and photographic infrared linear combinations for monitoring vegetation. *Remote Sens. Environ.* **1979**, *8*, 127–150. [CrossRef]
47. Hu, C. A novel ocean color index to detect floating algae in the global oceans. *Remote Sens. Environ.* **2009**, *113*, 2118–2129. [CrossRef]
48. Hang, X.; Li, X.; Li, Y.; Zhu, S.; Li, S.; Han, X.; Sun, L. High-Frequency Observations of Cyanobacterial Blooms in Lake Taihu (China) from FY-4B/AGRI. *Water* **2023**, *15*, 2165. [CrossRef]
49. Tu, Y.; Jia, K.; Wei, X.; Yao, Y.; Xia, M.; Zhang, X.; Jiang, B. A Time-Efficient Fractional Vegetation Cover Estimation Method Using the Dynamic Vegetation Growth Information from Time Series GLASS FAC Product. *IEEE Geosci. Remote Sens. Lett.* **2020**, *17*, 1672–1676. [CrossRef]
50. Yan, K.; Gao, S.; Chi, H. Evaluation of the Vegetation-Index-Based Dimidiate Pixel Model for Fractional Vegetation Cover Estimation. *IEEE Geosci. Remote Sens.* **2021**, *99*, 1–14. [CrossRef]
51. Riihimäki, H.; Luoto, M.; Heiskanen, J. Estimating fractional cover of tundra vegetation at multiple scales using unmanned aerial systems and optical satellite data. *Remote Sens. Environ.* **2019**, *224*, 119–132. [CrossRef]
52. Song, D.; Wang, Z.; He, T.; Wang, H.; Liang, S. Estimation and validation of 30 m fractional vegetation cover over China through integrated use of Landsat 8 and Gaofen 2 data. *Sci. Remote Sens.* **2022**, *6*, 100058. [CrossRef]
53. Wang, D.; Zhan, Y.; Yu, T.; Liu, Y.; Jin, X.; Ren, X.; Chen, X.; Liu, Q. Improving Meteorological Input for Surface Energy Balance System Utilizing Mesoscale Weather Research and Forecasting Model for Estimating Daily Actual Evapotranspiration. *Water* **2020**, *12*, 9. [CrossRef]
54. Dai, X.; Qian, P.; Ye, L.; Song, T. Changes in nitrogen and phosphorus concentrations in Lake Taihu, 1985–2015. *J. Lake Sci.* **2016**, *5*, 935–943.
55. Webster, I.T. Effect of wind on the distribution of phytoplankton cells in lakes revisited. *Limnol. Oceanogr.* **1994**, *39*, 365–373. [CrossRef]
56. Zhu, Y.; Cai, Q. The Dynamic Research of The influence of Wind Field on The Migration of Algae in Taihu Lake. *J. Lake Sci.* **1997**, *9*, 152–158.
57. Lu, W.; Yu, L.; Ou, X.; Li, F. Relationship between occurrence frequency of cyanobacteria bloom and meteorological factors in Lake Dianchi. *J. Lake Sci.* **2017**, *29*, 534–545.
58. Zhang, X.; Chen, Q. Spatial-temporal characteristic of water quality in Lake Taihu and its relationship with algal bloom. *J. Lake Sci.* **2011**, *23*, 339–347.
59. Zhang, Y.; Li, W.; Chen, Q. Spatial-temporal variance of the intensity of algal bloom and related environmental and ecological factors in Lake Taihu. *Acta Ecol. Sin.* **2016**, *36*, 4337–4345.
60. Guan, Q.; Feng, L.; Hou, X.; Schurgers, G.; Zheng, Y.; Tang, J. Eutrophication changes in fifty large lakes on the Yangtze Plain of China derived from MERIS and OLCI observations. *Remote Sens. Environ.* **2020**, *246*, 111890. [CrossRef]
61. Deng, K.; Liu, W.; Azorin-Molina, C.; Yang, S.; Li, H.; Zhang, G.; Minola, L.; Chen, D. Terrestrial stilling projected to continue in the Northern Hemisphere mid-latitudes. *Earth's Future* **2022**, *10*, e2021EF002448. [CrossRef]